ELSEVIER

Journal of Organometallic Chemistry 538 (1997) 151–161

Journal of Organometallic Chemistry

Photoactivated hydrosilation curing of a ceramic precursor: crosslinking and pyrolysis of branched oligo[(methylsilylene)methylene] [1]

Bryan E. Fry, Andrew Guo, D.C. Neckers *

Center for Photochemical Sciences, Bowling Green State University, Bowling Green, OH 43403, USA

Received 3 October 1996; revised 16 December 1996

Abstract

The complex *bis*(acetylacetonato)platinum(II) was activated by UV light in liquid mixtures of oligo[(methylsilylene)methylene] (OMSM) leading to rapid solidification and the formation of polycarbosilane with a crosslinked structure. A hydrosilation catalyst is produced by irradiation of this complex which promotes chain extension at OMSM silicon hydride sites with the additive tetravinylsilane. Dihydridosilicon end groups on the oligomer are necessary for rapid photocuring. The crosslinked polymers were pyrolyzed under inert conditions giving 70% yields of β-silicon carbide ceramic char with an overall carbon to silicon ratio of 1.79 to 1. Films of OMSM resin were spin-coated onto silicon wafers, cured, and pyrolyzed. Images on the film surfaces were retained in shape and dimension after pyrolysis. © 1997 Elsevier Science S.A.

1. Introduction

Silicon carbide ceramic can be derived from high temperature treatment of polymeric precursors containing polycarbosilane and polysilane backbones [1–3]. Fibers (or films) of the precursor are typically pyrolyzed at temperatures of 1000 °C or higher, under inert gas, leading to refractory ceramic fibers. Thus the precursor polymers are typically designed to be processed into fibers from a melt or solution, cured by thermal oxidation or UV exposure to set the material, and finally pyrolyzed.

Polycarbosilane precursors may be synthesized by several methods [4,5] including ring-opening polymerization of disilacyclobutanes bearing various functionalities, using a platinum catalyst. Linear polymers prepared in this manner by Wu and Interrante [6–8] with chloroplatinic acid gave ceramic yields of 66% for poly[(methylsilylene)methylene], $[-(CH_3)SiHCH_2-]_n$, and 87% for poly(silylenemethylene), $(-SiH_2CH_2-)_n$.

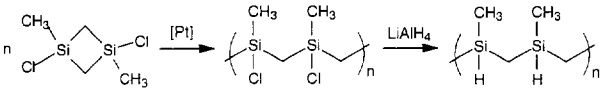

Polycarbosilane can also be produced from polydimethylsilane by Kumada rearrangement [9] at 470 °C as shown below. This is the method of Yajima, yielding 60% ceramic char after pyrolysis [10]. Poly(methylsilane) was used directly as a ceramic precursor [11,12]. The favorable stoichiometry of this polymer resulted in yields of 77% ceramic [13] with a final Si to C molar ratio near 1:1. Scarlete et al. coated silicon wafers with thin films of poly(methylsilane) and pyrolyzed them to produce semiconductor-grade SiC layers [14].

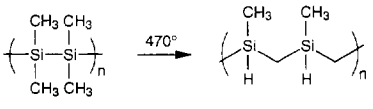

* Corresponding author.

[1] Contribution No. 281 from the Center for Photochemical Sciences.

PII S0022-328X(97)00042-9

Grignard coupling of (chloromethyl)chlorosilanes with magnesium turnings produces carbosilane polymers through initial formation of a Grignard reagent by reaction of chloromethyl groups with magnesium and subsequent attack on chlorosilicon moieties of surrounding monomers. Whitmarsh and Interrante synthesized highly branched polycarbosilane consisting entirely of head to tail coupling from (chloromethyl)trichlorosilane using this method [15].

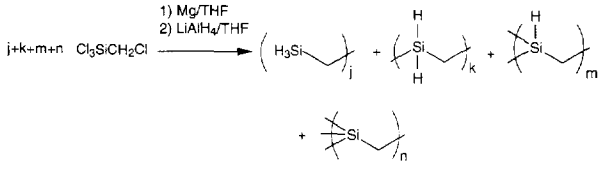

The ceramic yield from pyrolysis of linear poly(silylenemethylene) [8] is considerably higher (87%) than that from linear poly(vinylsilane) [16], $(-SiH_2CH_2CH_2-)_n$ (30–40%). Loss of ethylene was detected from the latter by mass spectrometry during pyrolysis indicating that excess carbon in the main chain is detrimental to ceramic yields [17]. The analogous dimethylsilyl compounds [17,18], $[-(CH_3)_2SiCH_2CH_2-]_n$ and $[-(CH_3)_2SiCH_2-]_n$, both gave negligible yields. The larger yields from the dihydridosilicon polymers are attributed to more favorable stoichiometry and to crosslinking by silylene species subsequent to hydrogen loss during pyrolysis [17].

Thorne et al. reported a high ceramic yield (85%) from ethynyl functionalized polycarbosilane fibers which were crosslinked by UV light prior to pyrolysis [19]. In this report the photolysis step was used to set the preformed fibers and prevent loss of shape during pyrolysis. Our objective was to use a photochemical step as the primary means of solidifying a liquid preceramic without the use of added solvents or melting. The report of a catalyst, *bis*(acetylacetonato)platinum(II) **1** or $Pt(acac)_2$, that was activated by UV light for hydrosilation addition reactions [20,21] and the rapid polymerization of vinyldimethylsilane [22] with $Pt(acac)_2$ prompted us to utilize it for crosslinking liquid preceramic polymers. Lewis et al. determined that absorption of UV light by **1** induces the cleavage of one ligand [23]; this is followed by complexation of olefins and silicon hydride groups at two active sites, thus forming a homogeneous hydrosilation catalyst. Subsequent bond cleavage of the remaining ligand by UV light absorption eventually leads to the formation of a heterogeneous platinum catalyst.

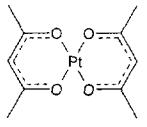

bis (acetylacetonato)platinum(II) 1

We have crosslinked branched oligo[(methylsilylene)methylene], $[-(CH_3)SiHCH_2-]_n$, (OMSM) in UV light using photoactivated $Pt(acac)_2$ to form solid polymer precursors which were then pyrolyzed under argon. We report here descriptions of this work and characterizations of the polymer and char product.

2. Results

2.1. Oligomer characteristics

OMSM was prepared by a Grignard coupling reaction followed by reduction as shown in Scheme 1. The product is complicated somewhat by the cleavage of THF and incorporation into the polymer. This is similar to the cleavage of diethyl ether previously reported during the synthesis of branched poly(silylenemethylene) [15].

This synthesis technique produced a broad range of oligomers with the smallest molecules consisting of trimers and tetramers, etc. Fig. 1, a gas chromatogram of the product mixture, reveals groups of isomers of lower oligomers ranging from three to seven units large. The mass spectral data is reported for selected trimers and tetramers (having sufficient signal intensity). The molecular ions for most of these match molecular weights of cyclic oligomers (or alkenes, which is unlikely). Indeed, Kriner used a technique similar to that of Scheme 1 to prepare cyclic dimers [24]. The mass fragments for trimer 1 and tetramer 4 correspond to uncyclized oligomers. [The highest mass listed for 1-trimer is M − 1. The highest mass fragment for 4-tetramer corresponds to M − Me ($m/e = 219$ plus isotopic contributions). The highest m/e for 8-tetramer is M − Me.] Examples of some postulated small oligomers produced in Scheme 1 are shown below (for $n = 3$ and 4 only). It

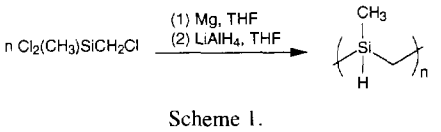

Scheme 1.

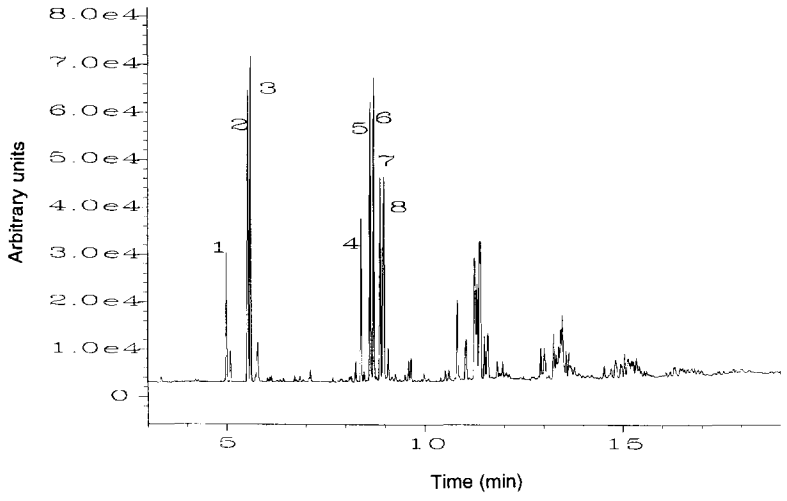

Fig. 1. Gas chromatogram of the oligomer product revealing small isomers with unit lengths of $n = 3$ to about $n = 7$. Mass spectral data for numbered components are reported in Section 4.

is assumed that cyclic dimers and trimers are incorporated into the larger oligomer chains as well.

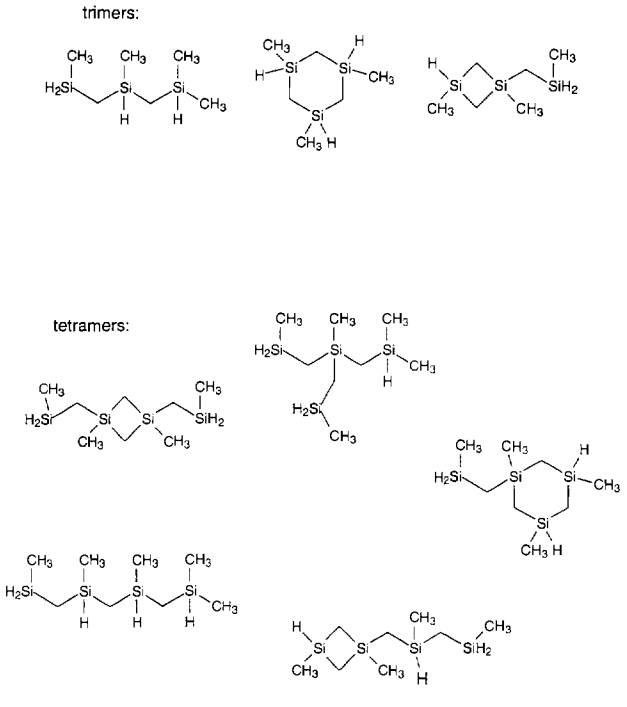

The ^{29}Si NMR spectrum, shown in Fig. 2(a), contains resonances due to tetraalkyl silicons, $(CH_3)Si(-CH_2-)_3$, near 2 ppm, silicon hydride, $(CH_3)SiH(-CH_2-)_2$, at about −16 ppm and silicon dihydride, $(CH_3)SiH_2(-CH_2-)$, near −38 ppm. Integration of the ^{29}Si NMR spectrum provided a means of analysis of the relative abundance of the three types of silicon centers in the OMSM. The results are shown in Table 1.

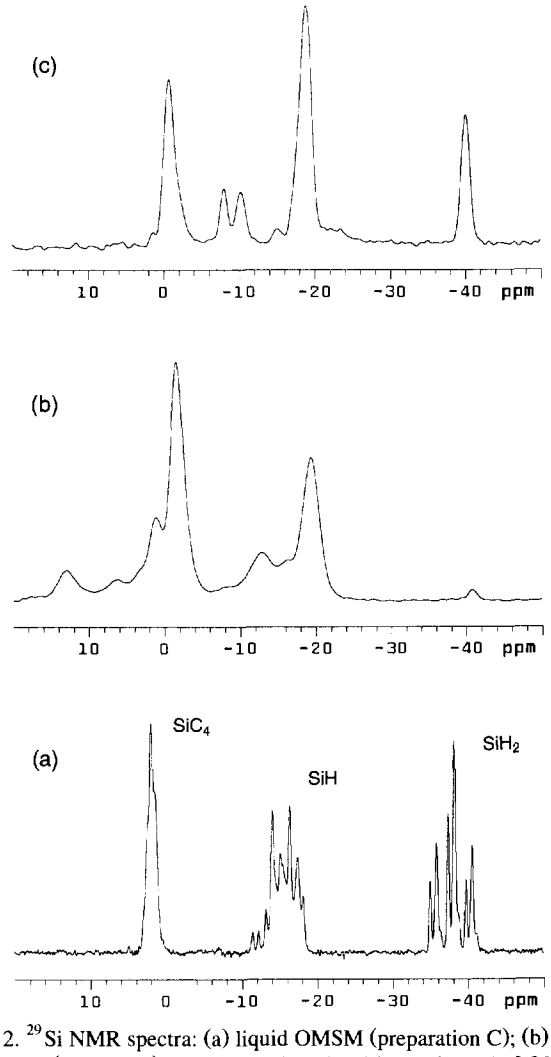

Fig. 2. ^{29}Si NMR spectra: (a) liquid OMSM (preparation C); (b) solid polymer (CP/MAS) photocrosslinked with TVS and 0.3% wt $Pt(acac)_2$; (c) solid polymer crosslinked by moisture without TVS. Chemical shifts are referenced to external TMS.

Table 1
Relative abundance of OMSM silicon atom types

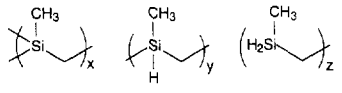

OMSM preparation	Ratio [a]		
	X	Y	Z
A	0.81	1.02	1.17
B	0.90	1.12	0.98
C	0.85	1.18	0.97

[a] Based on the ^{29}Si NMR peak area normalized to 3.

2.2. Photocrosslinking

OMSM mixed with tetravinylsilane (TVS) and $Pt(acac)_2$ was polymerized by UV irradiation, resulting in the formation of a hard and porous material. Without $Pt(acac)_2$ the OMSM did not solidify under UV irradiation. When TVS and $Pt(acac)_2$ without OMSM were irradiated no solids or non-volatile products were formed. Fig. 3 is a plot of gel time as a function of temperature. The polymerization rate increases, as indicated by lower gel times, at higher temperatures. Above 40 °C the gel time is relatively constant having nominal values of 10 to 13 min. At 70 °C and higher, $Pt(acac)_2$ is activated thermally without light, resulting in gelation. At 60 °C the samples did not gel within 30 min without light. Thus an optimum temperature range of about 40 to 60 °C was selected for rapid polymerization which could be controlled with light. Hydrogen bubbles formed during irradiation and remained encapsulated in the polymer after gelation of the sample. These bubbles are thought to result from silicon hydride reduction of the platinum and ligand during activation of the catalyst [25,26]. Low resolution images of crosslinked films of OMSM on silicon wafers were made and are shown in Fig. 4. Unlike the polymer plugs, irradiated films did not contain bubbles.

The solid-state ^{13}C NMR spectrum of the polymer produced by photoactivated crosslinking of OMSM with TVS was taken (not shown). This spectrum showed little change from the liquid OMSM ^{13}C spectrum other than downfield broadening during liquid to solid transformation, attributed to consumption of dihydride silicon groups and incorporation of vinyl crosslinks into the network [17,22]. There was no residual vinyl functionality visible in the spectrum of the solid.

The solid-state ^{29}Si NMR of the polymer, Fig. 2(b), shows a more dramatic change after crosslinking. The dihydride signal almost completely disappeared during the reaction while peaks from monohydridosilicon remained after crosslinking. The dihydride end groups

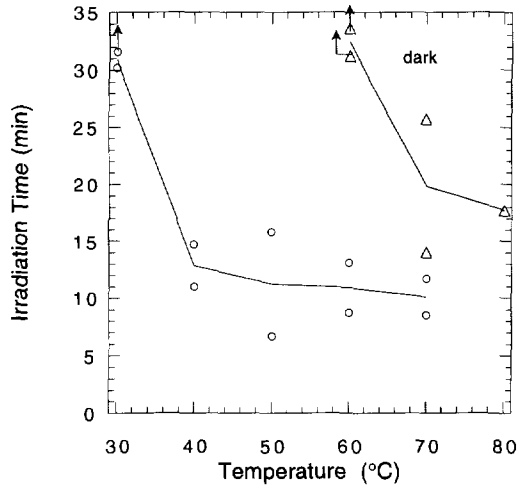

Fig. 3. Gel time of OMSM/TVS and 1% wt $Pt(acac)_2$: ○, irradiated; △, dark; ————, averages. Arrows denote samples which did not gel within the time specified by the data point.

were therefore the most reactive hydride functionality with the photoactivated catalyst. This observation is consistent with conclusions drawn by Lewis and Uriarte that addition of silicon monohydride to olefins proceeds more slowly than dihydride addition until all of the dihydride is consumed, after which the rate of the former increases [27].

The IR of the polymer shown in Fig. 5 displays some additional spectral changes from crosslinking. Evidence of the preferential consumption of SiH_2 is seen in the polymer IR spectrum by decrease of the band at 955 cm^{-1}, attributed to SiH_2 deformations [28]. The SiH stretching (2125 cm^{-1}) and bending (900 cm^{-1}) peaks diminish as well after crosslinking. This indicates that SiH groups reacted to some extent during the reaction. The 2125 cm^{-1} band shifted slightly to 2104 cm^{-1} for samples which were more extensively crosslinked (by post-curing). Since this peak arises from

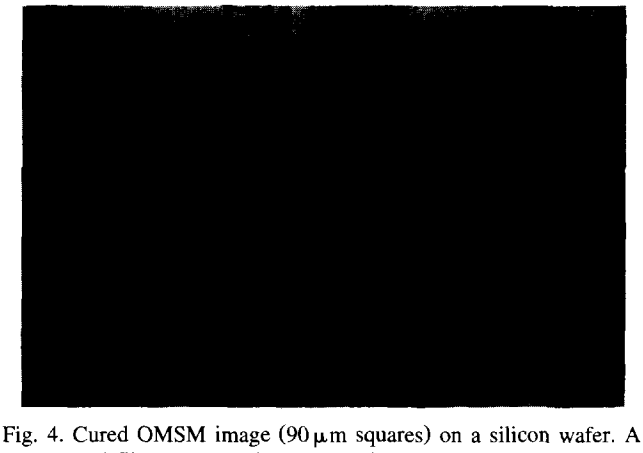

Fig. 4. Cured OMSM image (90 μm squares) on a silicon wafer. A spin-coated film of the resin was irradiated through a copper mask and rinsed with solvent afterwards. The area surrounding the squares is bare silicon. Rings which appear are caused by diffraction of light by the thin polymer film.

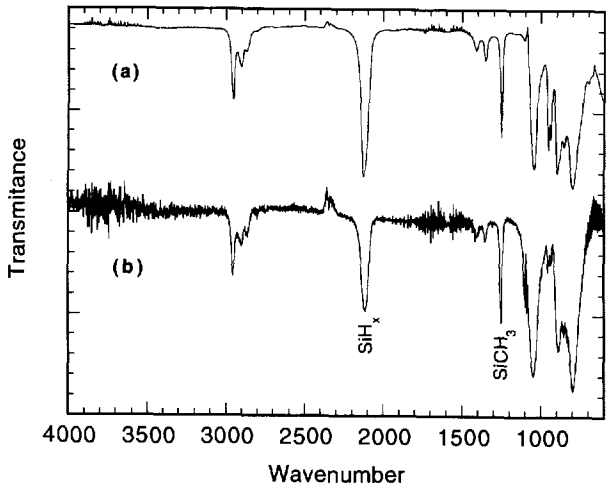

Fig. 5. Infrared spectra: (a) liquid OMSM; (b) spin-coated film of OMSM, TVS and 0.3% wt Pt(acac)$_2$ photocrosslinked by exposure to light for 120 s under dry air (normalized). The degree of SiH$_x$ conversion of the cured film is 52%.

stretching of both mono- and dihydride silicons and is thus a measure of both functionalities, the red shift is expected due to removal of the SiH$_2$ contribution during crosslinking [28]. A typical polymer plug sample irradiated for 8 min and kept at 50 °C for 22 min displayed 60% SiH$_x$ conversion based on IR results (not shown).

2.3. Polycarbosilane photocrosslinking

Commercial polycarbosilane (PCS) mixed with TVS and Pt(acac)$_2$ gelled very slowly compared to OMSM, such as to make it unsuitable for photoimaging. The mixtures did not gel with air present. This is similar to the results of Lewis and Salvi in which oxygen inhibited Pt(acac)$_2$ photocatalyzed addition reactions [20]. IR spectra showed slightly more SiH$_x$ conversion for degassed PCS mixtures than those prepared in air (23% and 17% respectively) 16 h after irradiation.

2.4. Effect of moisture

The OMSM crosslinking reaction proceeds with or without air when TVS is included, but in the absence of TVS crosslinking only occurs in air, not under argon. A side reaction with moisture is thought to be responsible for this. When dry air was bubbled through the samples without TVS no crosslinking took place upon irradiation. Injection of a few drops of water into these samples (post-irradiated) produced rapid curing along with bubbling. A solid-state ^{29}Si NMR spectrum of the moisture crosslinked polymer, Fig. 2(c), shows new peaks at δ −8.0 and −10.3 which may be explained by formation of Si–O–Si crosslinks as shown in Scheme 2 (^{29}Si NMR chemical shifts of or near δ −6.6 for (CH$_3$)*Si*H–O–Si were reported by Marsmann [29], see also Ref. [30]). Lestel et al. reported such a platinum catalyzed reaction between silicon hydrides and trace concentrations of water [30]. If this is the case, then silanol and hydrogen gas are formed from reaction of silicon dihydride OMSM end groups and water. The crosslinking is subsequently produced by condensation of the silanol with other silicon hydride groups. Polymerization of OMSM without TVS produces excessive bubbling resulting in foamy, fragile polymer.

2.5. Pyrolysis

Small plugs and powders of the crosslinked polymer were pyrolyzed under argon yielding black ceramic char products (70% wt). The polymer plugs retained their shape and texture throughout pyrolysis. This resulted in formation of porous material because of bubbles introduced during crosslinking. Fig. 6 illustrates the retention of polymer shape of a film of crosslinked OMSM pyrolyzed on a silicon wafer. Impressions of squares made on the film surfaces were not disturbed by the pyrolysis treatment.

DSC traces were featureless throughout the first heating (to 500 °C). The second heating though revealed endotherms at 476 °C. A TGA graph of the heating is shown in Fig. 7, which shows the onset of major weight loss at about 430 °C. An X-ray diffraction pattern of the char product, Fig. 8, is shown in comparison to that of commercial β-silicon carbide. The peak broadening of this data may result from crystal defects, anisotropy, or small crystal size. Assuming the latter explanation, the crystal size was calculated to be 24–28 Å. This is

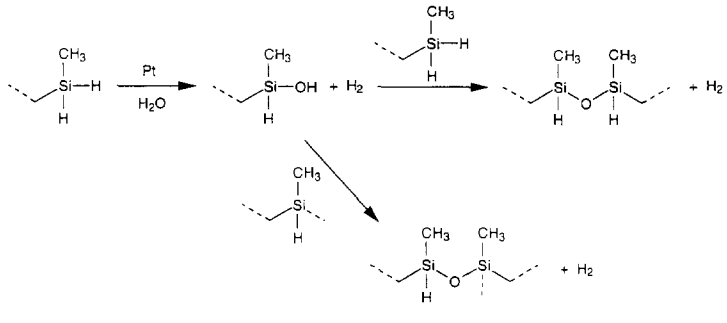

Scheme 2.

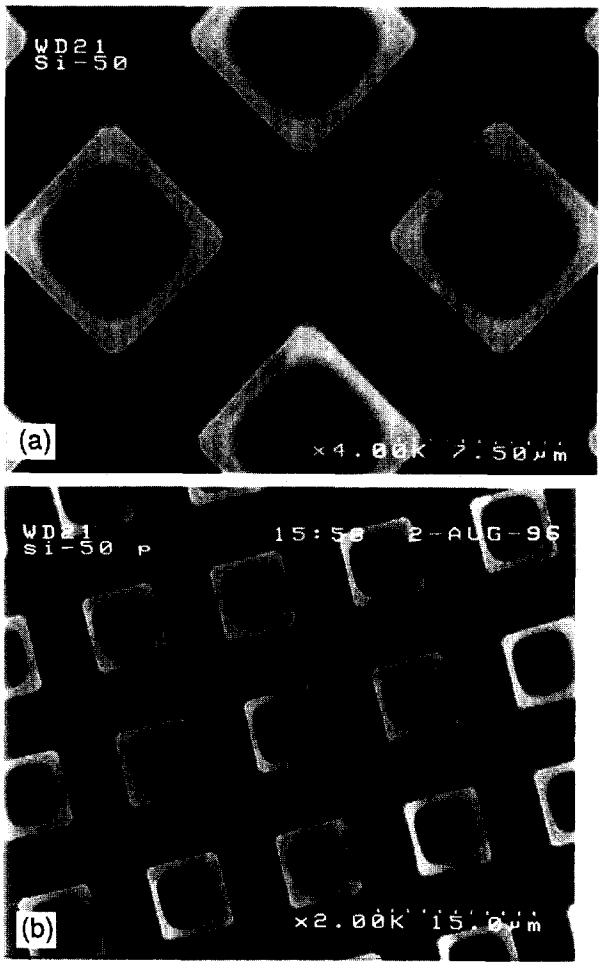

Fig. 6. SEM photos of an impression (9 μm squares) in cured OMSM resin on a silicon wafer. (a) Photocrosslinked film made using a 2000 mesh copper mask. The irradiation dose in this case was high enough to crosslink the entire surface. (b) The same surface shown after pyrolysis.

smaller than the values reported by Thorne et al. for crosslinked polycarbosilane containing methyl groups and pyrolyzed under similar conditions [19] (35 and 62 Å). The commercial silicon carbide shown (Fig. 8) has a calculated crystal size of 228 Å which is close to literature values [31].

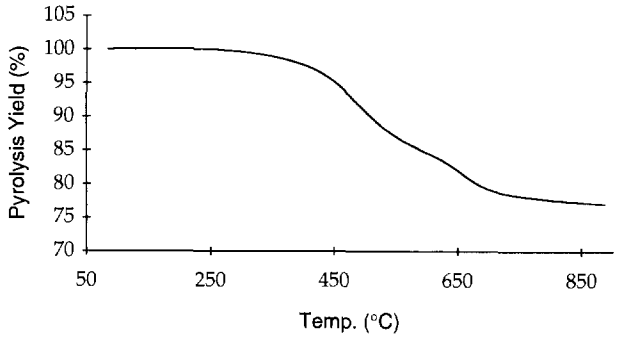

Fig. 7. Thermal gravimetric analysis of solid OMSM polymer photocrosslinked with TVS and 0.5% $Pt(acac)_2$.

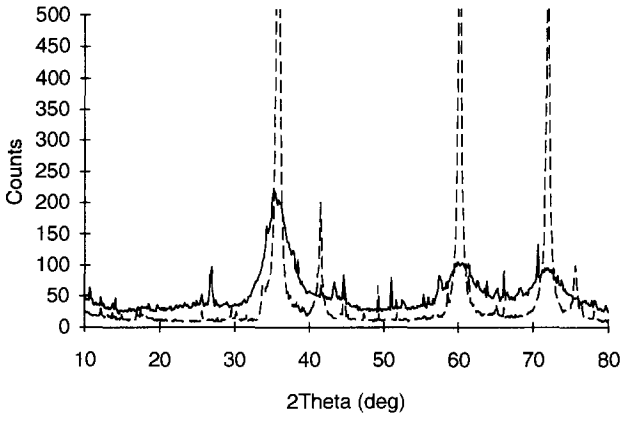

Fig. 8. X-ray diffraction patterns of: ———— char product of OMSM polymer photocrosslinked with TVS and 0.3% $Pt(acac)_2$; – – – commercial β-silicon carbide.

The molar ratio of carbon to silicon based on elemental analysis of the char (Section 4) is 1.79 to 1, so the ceramic contains a considerable amount of excess carbon. This analysis also leaves about 9% wt of the ceramic unaccounted for and presumably includes hydrogen, oxygen and a trace of platinum.

2.6. Catalyst photolysis

Spectral results in Fig. 9 show the photolytic disappearance of $Pt(acac)_2$ (344 nm peak) and the production of photoproduct (265 nm) using the additive vinyldimethylsilane. The quantum yields of photolysis with several additives are listed in Table 2. At fixed concentrations of oligomers or monomers the photolysis proceeds with higher quantum yields as the multifunctionality of reactive groups on silicon atoms increases. OMSM, containing both di- and monohydridosilicons, has an overall functionality of about 1 and promoted

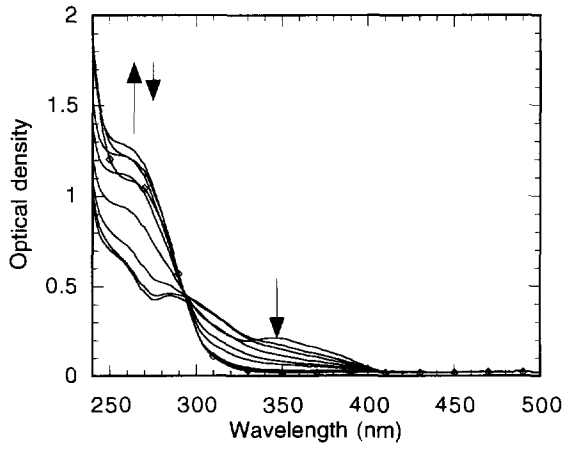

Fig. 9. Absorption spectra of the photolysis of 5×10^{-4} M $Pt(acac)_2$ with 0.5 M vinyldimethylsilane. Decay of the 344 nm peak is due to photodecomposition of catalyst. ———— 0, 1, 2, 4, 7, 10, 25, and 45 min, -◇-◇- 90 min.

Table 2
Quantum yields for the photolysis of $Pt(acac)_2$ with silicon hydride and olefin monomers

Additive [a]	Φ [b] $\times 10^3$	Active groups [c]
none [d]	0.047 ± 0.005	—
PCS	0.65 ± 0.04	≈ 0.6 [e]
OMSM	2.1 ± 0.04	≈ 1 [f]
Et_3SiH [g]	1.8	1
1-hexene [g]	2.6	1
VDMS	9.8 ± 0.06	2
TVS	14 ± 0.9 [h]	4

PCS = polycarbosilane, OMSM = oligo[(methylsilylene)methylene], VDMS = vinyldimethylsilane, TVS = tetravinylsilane.
[a] Concentration 0.4 M based on moles of silicon atoms.
[b] Error is standard deviation.
[c] Average number of olefin and silicon hydride groups per silicon atom or small molecule.
[d] 5.8×10^{-4} M $Pt(acac)_2$; photolyzed to 9% conversion.
[e] Based on ^1H NMR; see also Refs. [19,32].
[f] See Table 1.
[g] Values reported by Lewis et al. in Ref. [23].
[h] One of three samples photolyzed to 41% conversion.

catalyst reactivity similarly to triethylsilane and 1-hexene, reported previously [23]. Tetravinyl- and vinylhydridosilicon produced greater reactivity than did OMSM; PCS, with less than one reactive group per silicon, affected lower reactivity. No degassing was done for these experiments; Lewis et al. determined that even in cases where oxygen inhibited photocatalyzed hydrosilation reactions, it did not inhibit the photolytic conversion of $Pt(acac)_2$ to the active catalyst [23].

3. Discussion

UV light participates in the reaction only to activate the $Pt(acac)_2$ [20,22]. Once photoactivated, the catalyst mediates hydrosilation addition in the dark leading to crosslinking of OMSM. During UV irradiation $Pt(acac)_2$ undergoes Pt–O bond cleavage leading to a monodentate secondary photoproduct complexed with silicon hydride and olefin groups (Scheme 3). These reactive functionalities trap the primary ring-opened photoproduct, thus inhibiting the dark back reaction which regenerates $Pt(acac)_2$. This effect can be seen by the 1–2 order of magnitude increase in quantum yield when silicon hydride or olefin additives are present during photolysis (Table 2). The quantum yield is a measure of the trapping efficiency of the various additives. Molecules with larger numbers of complexing substituents are, therefore, better trapping agents.

While oxygen does not inhibit the formation of the secondary photoproduct, the subsequent hydrosilation addition of triethylsilane to olefins did not proceed in the presence of oxygen [20]. This was also observed in the crosslinking of commercial PCS. What these two reactants have in common is monohydridosilicons. Oxygen inhibited neither the crosslinking of OMSM, which contains approximately one third dihydridosilicons, nor polymerization of vinyldimethylsilane which also contains bifunctional silicons in terms of reactive functionalities [22]. This suggests that multiactive silicon centers may compete with oxygen more effectively than monoactive silicons for occupation of photogenerated platinum active sites.

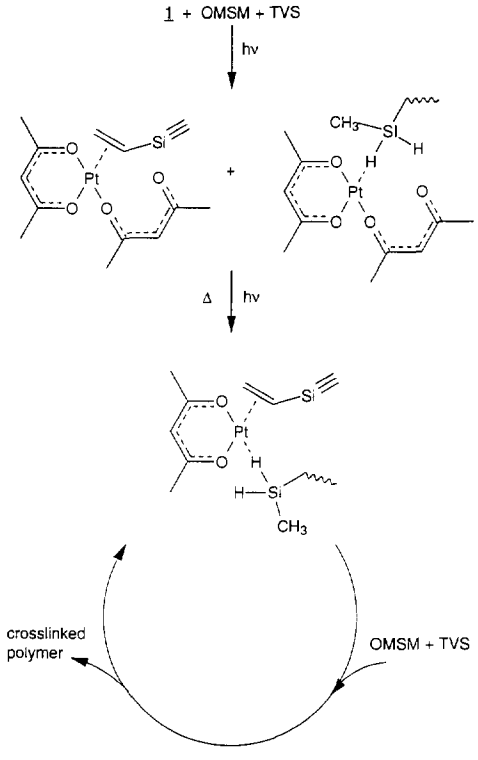

Scheme 3.

A mechanism of thermal activation was proposed by Lewis and coworker for generation of colloidal platinum catalysts from platinum complexes in which the ligand and metal of the starting complex are reduced by silicon hydride [25,33]. The bubbling observed during OMSM crosslinking, presumed to be hydrogen, suggests such a reduction. While $Pt(acac)_2$ is stable in the dark with OMSM, the primary photoproduct may be susceptible to spontaneous reduction by the dihydride moieties. Less powerful reducing agents such as monohydridosilanes might not accomplish the reduction in this system, thus requiring the second photon for catalyst activation as postulated by Lewis and Salvi [20].

The OMSM dihydridosilane groups were more readily consumed during the crosslinking reaction than were

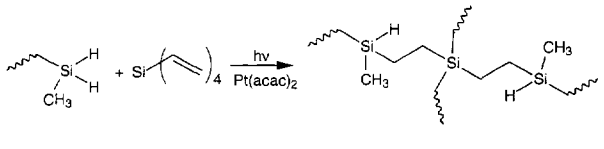

Scheme 4.

the monohydridosilane groups. This result suggests that the addition of silicon atoms to tetravinylsilane should occur primarily at the end groups of the branched oligomer, which are initially the dihydrides. Thus, chain extension of the pre-existing OMSM branches takes place as in Scheme 4. This occurs along with cross-linking at monohydrido sites.

The silicon carbide produced by this system was contaminated with excess carbon; this will lower the thermal stability of the material in high temperature applications. Further work is necessary to reduce the carbon to silicon ratio of the starting oligomers while retaining the favorable polymerization rate induced by the dihydridosilicon centers of OMSM.

4. Experimental

4.1. General

^{1}H and ^{13}C NMR spectra were obtained using a Varian Gemini 200. A Varian UnityPlus 400 NMR with a switchable probe or a room temperature CP/MAS probe was used to collect ^{29}Si liquid and solid-state spectra and ^{13}C solid-state NMR spectra. NMR solvents were purchased from Aldrich. These spectra were obtained as follows: ^{1}H at 200 MHz using 16–32 scans with a 5 s delay, $^{13}C\{^{1}H\}$ at 50.3 MHz using 256 scans with a 2 s delay, ^{29}Si at 79.5 MHz using 352 or more scans with a 50 s delay and ^{1}H decoupled only during the pulse. (The maximum standard deviation in peak integrated areas was $\pm 2.8\%$ between spectra with delays of 20 s, 30 s, 40 s, and 50 s. Removal of all decoupling has an insignificant effect on the integrated Si molar ratio.) CP/MAS experiments were done at spinning rates of 4000 Hz and contact times of 500 μs (^{13}C) and 1250 μs (^{29}Si) with 2000 scans. The solid polymer samples were crushed and packed into zirconium oxide NMR rotors.

Infrared spectroscopy of neat OMSM on NaCl plates (Aldrich), of crushed polymer pressed with oven dried KBr (FTIR grade, Aldrich) under argon, or of films on silicon wafers was done with a Mattson Galaxy 6020 spectrophotometer. The degree of SiH_x conversion was determined by calculating the decrease in the integrated area of the 2125 cm^{-1} peak normalized by the area of the $SiCH_3$ deformation peak at 1253 cm^{-1} after photolysis.

A Hewlet Packard (HP) 5890 gas chromatograph with a 30 m × 0.253 mm ID × 0.25 μm film thickness DB-1 column (J&B Scientific) and a flame ionization detector was used to analyze low boiling oligomers. Also, an HP 5880 gas chromatograph with a 30 m × 0.25 mm ID × 0.25 μm film thickness DB-5ms column (J&B Scientific) coupled to an HP 5987A mass spectrometer was used to determine lower oligomer molecular weights. Overall oligomer molecular weights were determined by gel permeation chromatography with an HP 1050 series HPLC equipped with a 1047A refractive index detector and a PLgel 5 μm Mixed-C column. The solvent was THF at a flow rate of 0.80 ml min^{-1} and at 30 °C. An 11 point calibration curve was composed with polystyrene standards (Polysciences).

The gel time for photocrosslinking of the oligomers was measured with a prototype Gel-Pointe gelometer (described in Ref. [34]) with a quartz–halogen lamp and a thermostated temperature control. The Pyrex-filtered light intensity was 36 mW cm^{-2}. These samples were irradiated in Pyrex 10 μl capillary pipettes while the oscillatory response was outputted to a strip-chart recorder to determine gel time. Some gel time control experiments were performed with the lamp turned off and the capillary oven at temperatures from 60 to 80 °C to determine the reactivity of the catalyst without light.

Differential scanning calorimetry was performed using a Perkin Elmer DSC-4 with a glovebox and an intracooler. This instrument was calibrated with indium. For typical DSC runs, samples were placed in stainless steel pans under argon and heated from 25 to 500 °C at rates of 5 or 10 °C min^{-1} with an empty pan as reference. Two heating runs were conducted on each sample and samples were cooled at a rate of approximately 320 °C min^{-1} between runs. The thermal gravimetric analysis was performed at the University of Michigan on a TGA Hi-Res 2950 under argon.

X-ray diffraction of the polymer char products was determined by a Philips diffractometer with a PW1710 based control at a step size $[2\theta] = 0.02°$ and a PW1830 generator utilizing the Cu Kα line at 45 kV and 40 mA. The char material for X-ray analysis was finely ground in a ruby mortar and pestle and packed into flat specimen holders. β-Silicon carbide purchased from Alfa (1 micron) was used as a comparison standard. The full-width at half-height of the 35.7° (2.51 Å) β-silicon carbide peaks was measured and crystal sizes were estimated using the Scherrer formula [35].

Incident light intensity was measured with a Scientech 365 power and energy meter. Absorption spectroscopy was performed with an HP 8452A spectrophotometer. Microscopy was done on a Hitachi S-2700 scanning electron microscope at 15 kV and on a Zeiss optical microscope (256 ×).

Elemental analysis of the oligomer was performed by Quantitative Technologies, Inc., Whitehouse, NJ. Elemental analysis of the char product was performed by XRAL Ltd., Don Mills, Ont., Canada.

4.2. OMSM synthesis

THF solvent was passed through an activated alumina column, refluxed with $LiAlH_4$, and fractionated before use. In some cases the THF was distilled after

refluxing with sodium and benzophenone until a blue solution appeared. The product was not altered in either case. Magnesium turnings were baked at 130 °C overnight and freshly ground by mortar and pestle prior to use. The glassware used for synthesis was treated with a 5% solution of dichlorodimethylsilane in toluene, oven dried, and backfilled with dry argon or nitrogen before use.

The OMSM was synthesized by the method of Froehling [36]. (Chloromethyl)dichloromethylsilane was purchased from Aldrich and used as received. The reaction mixtures were refluxed for 2 h (preparation A) or 18 h (preparation B). The product was unaffected by the use of 4% vs. 10% HCl during workup.

^{1}H NMR (C_6D_6): δ −0.2 to 0.45 (broad m, 5 H, CH_3, CH_2), δ 4.07 (m, SiH_2), δ 4.33, 4.5, 4.9, 5.07 (m, SiH); combined SiH and SiH_2 peaks yield 1 H. Minor peaks attributed to THF cleavage products appear at δ 1.41, 3.35, and 3.61. ^{13}C NMR (C_6D_6): δ −5 (CH_3SiH_2), δ −1 (CH_3SiH), δ 1 to 9 (CH_2); these are broad peak centers containing multiple peaks. Peaks due to THF cleavage products appear at δ 14.3, 14.7, 23, 32.1, 35.5, 36.7, 37, and 62.5. ^{29}Si NMR (C_6D_6): δ −38 (m, SiH_2), δ −18, −16, −14 (m, SiH), δ 2, 3 (m, $Si(CH_x)_4$), δ −9 to −4 (minor), δ 6 to 9 (minor). UV/vis: $\lambda_{max} = 196$ nm, $a = 61\,g^{-1}\,cm^{-1}$. The GPC molecular weight distribution revealed two fractions which were not separated: preparation A, $M_w = 810$, $M_n = 610$ (73%) and $M_w = 32000$, $M_n = 17400$ (27%); preparation B, $M_w = 590$, $M_n = 440$ (65%) and $M_w = 51700$, $M_n = 16000$ (35%). Anal. Found: C, 42.72; H, 9.95; Cl, 0.38. Calc.: C, 41.30; H, 10.40, Si, 48.30% based on the average structure –$(CH_3)SiHCH_2$–.

In a third variation of the synthesis (preparation C) the reactants were refluxed for 18 h and the reduction and workup procedures were performed twice. The product was then eluted through a neutral alumina column with hexanes, dried by rotary evaporation, and pumped for 2 h under vacuum (< 1 mmHg) at 50 °C. Minor components which produced ^{29}Si NMR peaks at δ −9 to −4 and 6 to 9 ppm were removed by this procedure.

^{1}H NMR ($CDCl_3$): δ −0.15, 0.05 to 0.45 (broad m, 5 H, CH_3, CH_2), δ 3.82 (m, SiH_2), δ 4.06 (m, SiH); combined SiH and SiH_2 peaks yield 1 H. Minor peaks attributed to THF cleavage products appear at δ 1.42, 1.58, and 3.65. ^{13}C NMR (C_6D_6): δ −6 to −4 (CH_3SiH_2), δ −2 to 6 (CH_3SiH and CH_2); multiple peaks in these regions. Peaks due to THF cleavage products appear at δ 14.9, 15.3, 21, 36.6, and 62.3. Preparation C (g mol^{-1}), $M_w = 490$, $M_n = 440$ (52%) and $M_w = 36500$, $M_n = 24800$ (48%).

4.3. Lower oligomer mass spectral data

Isomers giving sufficient signal for identification are listed below (see Fig. 1 chromatogram). These were not separated from the higher molecular weight polymer. 1-Trimer: 175, 14.1%; 161, 50.7%; 117, 78.3%; 73, 100%; 59, 82.3%; 45, 43.4%. 2-Trimer: 174, 20.6%, M + ; 173, 20.5%; 159, 100%; 157, 23.7%; 129, 16.2%; 115, 15.1%; 113, 14.2%; 99, 19.3%; 85, 11.5%; 73, 26.2%; 59, 30.4%; 43, 21.0%. 3-Trimer: 174, 18.2%, M + ; 173, 17.4%; 159, 100%; 157, 32.2%; 129, 17.4%; 115, 17.4%; 99; 17.4%; 85, 17.1%; 73, 23.5%; 59, 21.3%; 43, 27.0%. 4-Tetramer: 221, 8.0%; 220, 12.8%; 219, 47.1%; 175, 96.6%; 159, 67.8%; 116, 11.4%; 103, 30.1%; 85, 20.4%; 73, 100%; 59, 56.6%; 43, 25.1%. 5-Tetramer: 232, 15.0%, M + ; 231, 11.2%; 217, 100%; 187, 17.3%; 173, 69.8%; 157, 57.2%; 143, 21.8%; 129, 18.7%; 115, 30.6%; 101, 26.4%; 99, 30.2%; 85, 24.2%; 73, 68.6%; 59, 69.0%; 43, 25.0%. 6-Tetramer: 232, 25.0%, M + ; 231, 9.8%; 217, 100%; 187, 28.5%; 173, 55.3%; 157, 41.5%; 143, 19.2%; 129, 15.8%; 115, 22.0%; 101, 26.8%; 85, 22.3%; 73, 51.5%; 59, 36.3%; 43, 30.1%. 7-Tetramer: 232, 10.2%, M + ; 231, 3.3%; 217, 68.3%; 173, 100%; 157, 52.9%; 143, 16.9%; 115, 27.8%; 101, 29.6%; 99, 27.1%; 85, 14.7%; 73, 49.6%; 59, 48.6%; 43, 25.1%. 8-Tetramer: 217, 49.7%; 173, 100%; 157, 39.2%; 143, 20.8%; 113, 26.1%; 101, 17.8%; 99, 17.8%; 85, 21.2%; 73, 57.9%; 59, 55.6%; 43, 30.3%.

4.4. Irradiation curing

The apparatus used for irradiation is shown in Fig. 10 and utilizes an Oriel 66002 illuminator with a 200 W Hg lamp collimated by a lens through a cooled IR water filter and a 300–400 nm bandpass filter. The beam is directed vertically by an Oriel 12620 mirror through the window of a sealed, thermostatically controlled oven with a black inner surface and fitted with ports for gas purging. The oven window is a 340 nm cutoff filter (Oriel 59460) thus providing irradiation to the sample at $\lambda_{max} = 368$ nm and at a power of 24 mW cm^{-2}.

Tetravinylsilane (TVS) was purchased from Aldrich or Gelest and used without further purification. A typical sample preparation consisted of 0.154 g of OMSM (2.6 mmol Si units) mixed with 0.054 g of TVS (0.40 mmol) measured into fluted aluminum foil cups. Under dim lighting 1 mg (0.5% wt) of finely ground Pt(acac)$_2$ (Alfa) was added to the mixture and stirred

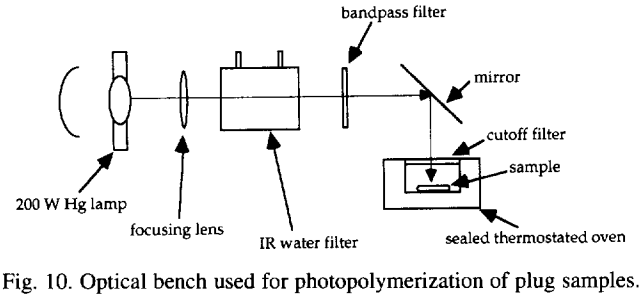

Fig. 10. Optical bench used for photopolymerization of plug samples. Incident light $\lambda_{max} = 368$ nm.

carefully before placing into the optical bench oven. $Pt(acac)_2$ has a low solubility in OMSM and TVS until irradiation is initiated. A few samples were prepared under dry argon and irradiated without admitting air. Several samples of OMSM were polymerized without TVS. The mixtures were typically irradiated for 8 min at 50 °C and allowed to remain in the oven for an additional 22 min to harden the polymer sufficiently to remove it from the foil cup. The polymer products were stored in a dessicator.

4.5. Thin film curing

Silicon wafers of about $1.5 \times 1.5\,cm^2$ were spin coated with the OMSM/TVS/$Pt(acac)_2$ mixture. Images and impressions were formed on some samples by placing 200 or 2000 mesh copper masks onto the film surfaces before irradiation. The coated wafers were irradiated for 30–120 s in the optical bench oven at 40 °C under dry air purging. For these experiments the optical bench filters were replaced with a single filter (Oriel 59425) providing illumination at > 300 nm and $0.40\,W\,cm^{-2}$. Immediately following the photocure, the wafers were rinsed several times with benzene to remove the mask and unreacted resin.

4.6. Moisture effect and commercial PCS curing

The effects of dissolved air and moisture on the polymerization were determined with OMSM and $Pt(acac)_2$. These mixtures were prepared with and without TVS in vials and irradiated with a dental lamp (> 300 nm) for 1–3 min. The vials were capped with septa and bubbled with dry argon or dry air before irradiation. Droplets of water were injected into some samples. The lamp was a Demetron model VCI 401 which produced borosilicate glass filtered light at about $1.2\,W\,cm^{-2}$. The entire beam of the lamp was directed into the bottoms of the vials.

Commercial polycarbosilane (PCS) powder was purchased from Nippon Carbon Co. and used without further purification ($M_n = 2440\,g\,mol^{-1}$). PCS (0.4 g) was dissolved in a minimum amount of $CHCl_3$ (0.5 g) and mixed with TVS (0.04 g) and $Pt(acac)_2$ (3 mg) in vials. Samples were capped with septa, bubbled with solvent saturated argon, and irradiated for 20 min using the dental lamp. These mixtures gelled about 24 h after irradiation. Some samples were not degassed and did not gel.

4.7. Quantum yield determination

$Pt(acac)_2$ solutions in dichloromethane with silane additives were irradiated on an optical bench at $\lambda_{max} =$ 368 nm. For these experiments the mirror and oven of the setup in Fig. 10 were replaced by a cuvette holder. Quartz cuvettes (Spectrocell) capped with septa were used; the cell holder was maintained at 25 °C by a Lauda circulating bath, and the solutions were magnetically stirred during irradiation. The decrease in $Pt(acac)_2$ concentration was measured by the change in optical density at 368 nm. Unless otherwise stated, the initial $Pt(acac)_2$ concentration was 5.5×10^{-4} M. These experiments were performed in triplicate and photolyzed to 22–27% conversion.

$Pt(acac)_2$ was dried in a vacuum desiccator at 50 °C prior to use and dichloromethane (Aldrich, spectral grade) was eluted through a column of basic alumina, refluxed over $LiAlH_4$, and fractionated prior to use. A stock solution of catalyst was prepared in red actinic glassware and diluted to the proper concentration before runs. The following additives were used: vinyldimethylsilane (preparation previously described [22]), TVS, OMSM, and PCS.

The absorbed light intensity was determined using a benzophenone/benzhydrol actinometer [37]. Benzophenone (BP) and benzhydrol (BH) were purchased from Fisher and Baker accordingly. Benzene solvent was Aldrich HPLC grade. These reagents were used without further purification. The BP concentration was adjusted to absorb the same amount of light as the sample solutions at 368 nm (95–97%). The actinometer solutions were degassed by bubbling with benzene saturated argon for 15 min. The quantum yield of the actinometer solution (0.021 M BP and 0.021 M BH) was 0.50 ± 0.05. The solutions were photolyzed to 18–23% conversion and were run in triplicate.

4.8. Pyrolysis

The crosslinked polymers were pyrolyzed at 1200 °C for 4 h. A preliminary group of polymer plugs was packed individually in carbon crucibles filled with boron nitride powder to support the samples. The furnace (Astro Industries, Inc. model 1000-4560-FP20) was backfilled with argon and maintained at a pressure of 5–10 psi throughout pyrolysis. The furnace temperature was increased at roughly $5\,°C\,min^{-1}$; cooldown was not carefully controlled. This technique gave ceramic yields of only about 50% wt. Yields of 70% wt were obtained from polymer samples placed on graphite foil lined alumina boats in quartz tubes and pyrolyzed in Lindberg tube furnaces under flowing argon ($100\,cc\,min^{-1}$). These ovens were heated at $2\,°C\,min^{-1}$ and cooled at $10\,°C\,min^{-1}$. Silicon wafers bearing crosslinked polycarbosilane films were pyrolyzed in Lindberg tube furnaces under flowing argon heating at $10\,°C\,min^{-1}$ from ambient up to 250 °C, at $2\,°C\,min^{-1}$ from 250 to 900 °C, and at $5\,°C\,min^{-1}$ from 900 to 1200 °C. The furnace cooldown rate was $10\,°C\,min^{-1}$.

The elemental analysis found for the ceramic product (average of two analyses) is C, 39.3; Si, 51.4 and Cl, 0.398%.

5. Conclusions

A polymer preceramic system utilizing the catalyst *bis*(acetylacetonato)platinum(II) was developed which allows a liquid oligocarbosilane mixture to be solidified by intense UV irradiation within about a minute. This polymer produces a high ceramic yield when pyrolyzed, retaining its shape and texture. Thin layers of silicon carbide on silicon wafers may be produced by this system. The char material consists mainly of β-silicon carbide and carbon. Dihydridosilicon OMSM end groups are critical to the rapid photoactivation of the catalyst and rapid crosslinking thereafter.

Acknowledgements

We are grateful to Dr. Richard M. Laine, Mark Nickanicky, Dr. John W. Halloran, and Gabriel Chu of the University of Michigan Dept. of Materials Science and Engineering for doing the TGA and pyrolysis work and for helpful discussions regarding ceramics and preceramics. This research was supported by the Harold and Helen McMaster Endowment, the Office of Naval Research (N00014-93-1-0772), the National Science Foundation (DMR-9013109), and the Edison Industrial Systems Center. The authors are grateful to each of these agencies and donors.

References

[1] K.J. Wynne and R.W. Rice, *Ann. Rev. Mater. Sci., 14* (1984) 297.
[2] R.M. Laine and F. Babonneau, *Chem. Mater., 5* (1993) 260.
[3] M. Birot, J.P. Pillot and J. Dunoguès, *Chem. Rev., 95* (1995) 1443.
[4] L.V. Interrante, Q. Liu, I. Rushkin and Q. Shen, *J. Organomet. Chem., 521* (1996) 1; L.V. Interrante, C.W. Whitmarsh, W. Sherwood, H.-J. Wu, R. Lewis and G. Maciel, in J.F. Harrod and R.M. Laine (eds.), *Applications of Organometallic Chemistry in the Preparation and Processing of Advanced Materials*, NATO ASI Series 297 (E), Kluwer Academic, Dordrecht, 1995, p. 173.
[5] E. Bacqué, M. Birot, J.P. Pillot, P. Lapouyade, P. Gerval, C. Biran and J. Dunoguès, *J. Organomet. Chem., 521* (1996) 99.
[6] H.J. Wu and L. Interrante, *Chem. Mater., 1* (1989) 564.
[7] H.J. Wu and L. Interrante, *Polym. Prepr., 32* (1991) 588.
[8] H.J. Wu and L. Interrante, *Macromolecules, 25* (1992) 1840.
[9] K. Shiina and M. Kumada, *J. Org. Chem., 23* (1958) 139.
[10] Y. Hasegawa, M. Iimura and S. Yajima, *J. Mater. Sci., 15* (1980) 720.
[11] D. Seyferth, in J.M. Zeigler and F.W.G. Gearon (eds.), *Silicon-Based Polymer Science*, Advances in Chemistry 224, American Chemical Society, Washington, DC, 1990, Chap. 31.
[12] D. Seyferth, G.H. Wiseman, J.M. Schwark, Y.-F. Yu and C.A. Poutasse, in M. Zeldin, K.J. Wynne and H.R. Allcock (eds.), *Inorganic and Organometallic Polymers*; ACS Symposium Series 360, American Chemical Society, Washington, DC, 1988, Chap. 11.
[13] Z.-F. Zhang, Y. Mu, F. Babonneau, R.M. Laine, J.F. Harrod and J.A. Rahn, in J.F. Harrod and R.M. Laine (eds.), *Inorganic and Organometallic Oligomers and Polymers*, Kluwer, Dordrecht, 1991, p. 127.
[14] M. Scarlete, I.S. Butler and J.F. Harrod, *Chem. Mater., 7* (1995) 1214.
[15] C.K. Whitmarsh and L.V. Interrante, *Organometallics, 10* (1991) 1336.
[16] B. Boury, R.J.P. Corriu, D. Leclercq, P.H. Mutin, J.M. Planeix and A. Vioux, *Organometallics, 10* (1991) 1457.
[17] R.J.P. Corriu, D. Leclercq, P.H. Mutin, J.M. Planeix and A. Vioux, *Organometallics, 12* (1993) 454.
[18] D. Seyferth and H. Lang, *Organometallics, 10* (1991) 551.
[19] K.J. Thorne, S.E. Johnson, H. Zheng, J.D. Mackenzie and M.F. Hawthorne, *Chem. Mater., 6* (1994) 110.
[20] F.D. Lewis and G.D. Salvi, *Inorg. Chem., 34* (1995) 3182.
[21] J.D. Oxman and L.D. Boardman, *Eur. Pat. Appl. 398,701*, 1990.
[22] B.E. Fry and D.C. Neckers, *Macromolecules, 29* (1996) 5306.
[23] F.D. Lewis, A.M. Miller and G.D. Salvi, *Inorg. Chem., 34* (1995) 3173.
[24] W.A. Kriner, *J. Org. Chem., 29* (1964) 1601.
[25] L.N. Lewis, *J. Am. Chem. Soc., 112* (1990) 5998.
[26] L.N. Lewis and N. Lewis, *Chem. Mater., 1* (1989) 106.
[27] L.N. Lewis and R.J. Uriarte, *Organometallics, 9* (1990) 621.
[28] G. Socrates, *Infrared Characteristic Group Frequencies*, Wiley, Chichester, UK, 2nd edn., 1994, pp. 188–194.
[29] M. Marsmann, in P. Diehl, E. Fluck and R. Kosfeld (eds.), *NMR Basic Principles and Progress*, Vol. 17, Springer, Berlin, 1981, p. 205.
[30] L. Lestel, H. Cheradame and S. Boileau, *Polymer, 31* (1990) 1154.
[31] K.R. Carduner, S.S. Shinozaki, M.J. Rokosz, C.R. Peters and T.J. Whalen, *J. Am. Ceram. Soc., 73* (1990) 2281.
[32] S. Yajima, Y. Hasegawa, J. Hayashi and M. Iimura, *J. Mater. Sci., 13* (1978) 2569.
[33] L.N. Lewis and N. Lewis, *J. Am. Chem. Soc., 108* (1986) 7228.
[34] E.J. Saccocio, *Radtec Report*, November/December 1990, p. 16.
[35] B.D. Cullity, *Elements of X-Ray Diffraction*, Addison-Wesley, Reading, 1956, p. 99.
[36] P.E. Froehling, *J. Inorg. Organomet. Polym., 3* (1993) 251.
[37] W.M. Moore and M. Ketchum, *J. Am. Chem. Soc., 84* (1962) 1368; S.L. Murov, *Handbook of Photochemistry*, Marcel Dekker, New York, 1973, pp. 125–126.